



Published in final edited form as:

*Anal Chem.* 2010 December 1; 82(23): 9892–9900. doi:10.1021/ac102399n.

## Characterization of Local pH Changes in Brain Using Fast-Scan Cyclic Voltammetry with Carbon Microelectrodes

Pavel Takmakov<sup>a</sup>, Matthew K. Zachek<sup>b</sup>, Richard B. Keithley<sup>a</sup>, Elizabeth Bucher<sup>a</sup>, Gregory S. McCarty<sup>b</sup>, and R. Mark Wightman<sup>a,\*</sup>

<sup>a</sup> Department of Chemistry, University of North Carolina at Chapel Hill, Chapel Hill, NC 27599, United States

<sup>b</sup> Department of Biomedical Engineering, University of North Carolina at Chapel Hill, North Carolina State University, Raleigh, NC 27607, United States

### Abstract

Transient local pH changes in the brain are important markers of neural activity that can be used to follow metabolic processes that underlie the biological basis of behavior, learning and memory. There are few methods that can measure pH fluctuations with sufficient time resolution in freely moving animals. Previously, fast-scan cyclic voltammetry at carbon-fiber microelectrodes was used for the measurement of such pH transients. However, the origin of the potential dependent current in the cyclic voltammograms for pH changes recorded *in vivo* was unclear. The current work explored the nature of these peaks and established the origin for some of them. A peak relating to the capacitive nature of the pH CV was identified. Adsorption of electrochemically inert species, such as aromatic amines and calcium could suppress this peak, and is the origin for inconsistencies regarding *in vivo* and *in vitro* data. Also, we identified an extra peak in the *in vivo* pH CV relating to the presence of 3,4-dihydroxyacetic acid (DOPAC) in the brain extracellular fluid. To evaluate the *in vivo* performance of the carbon-fiber sensor, carbon dioxide inhalation by an anesthetized rat was used to induce brain acidosis induced by hypercapnia. Hypercapnia is demonstrated to be a useful tool to induce robust *in vivo* pH changes, allowing confirmation of the pH signal observed with FSCV.

### Keywords

pH sensor; carbon-fiber microelectrode; *in vivo* voltammetry; hypercapnia; acidosis; adsorption; FSCV

## INTRODUCTION

Tight regulation of tissue pH is essential for living organisms<sup>1</sup>. The homeostatic value of pH represents a compromise between a multitude of processes that either generate, or consume both acidic and basic species. The most important factors in pH control are the processes of energy conversion and respiration. In higher-order mammals the brain consumes the most energy of any organ, accounting for up to 25% of the total metabolic energy expenditure<sup>2</sup>. This large energy demand can be accomplished only through the fast delivery of nutrients and soluble gasses, such as oxygen. Besides sizable energy requirements, the brain also requires approximately 20% of the cardiovascular output<sup>2</sup>. Neural activity is heterogeneous throughout the brain, and localized activation of certain

\*CORRESPONDING AUTHOR rmw@unc.edu.

brain regions will increase the local rate of metabolism, and subsequently local cerebral blood flow<sup>2</sup>. This link between region specific neural activity and the increase in regional consumption of nutrients (glucose) and oxygen is the basis for numerous brain imaging techniques such as blood oxygenation level dependent functional magnetic resonance imaging (BOLD fMRI) and positron emission tomography (PET)<sup>2</sup>. Monitoring pH in an intact brain, therefore, could provide important information regarding the mechanisms of metabolism and blood flow.

There are two major counteracting processes that control pH in the brain. Generally, metabolism involves the utilization of glucose either aerobically, with production of carbon dioxide, or anaerobically with production of lactic acid and carbon dioxide. The production of these species results in an acidic pH shift<sup>2-4</sup>. In concert with metabolism, a spike in neural activity causes an increase in local blood flow that facilitates the clearance of carbon dioxide, which is expired through the respiratory system<sup>5</sup>, leading to local alkaline pH shifts. The rapid dynamics of metabolism and carbon dioxide clearance suggests that local changes in pH can be used as a measurement of regional neural activity, which could help understand biological bases of behavior<sup>6,7</sup>. This opportunity provides the motivation for the development of a technique for accurate and spatially precise measurements of pH in the brain of freely moving animals.

There are several types of existing analytical methods for *in vivo* pH measurements<sup>8</sup>. The first group of techniques consists of spectroscopic methods based on pH-induced changes in absorbance or fluorescence of pH sensitive dyes, or on the chemical shifts in nuclear magnetic resonance (NMR) signal for phosphorus in phosphate groups<sup>2</sup>. Methods based on spectroscopy in the visible spectrum are widely used for *in vitro* studies, but they are less convenient to use for *in vivo* pH measurements. NMR based imaging has the advantage of being non-invasive, however, in animal experiments NMR does not allow for behavioral paradigms that require unrestricted animal movement.

The second group of methods is based on potentiometric measurements, implementing pH-sensitive microelectrodes. These ion-selective sensors are in the form of either glass microelectrodes<sup>9</sup> or solid state microelectrodes based on metal oxides with iridium oxide being the most popular<sup>10</sup>. These methods are advantageous for *in vitro* tissue preparations where the chemical composition of the solution can be controlled. However, the transfer of these techniques for pH measurements in freely moving animals is problematic. Glass microelectrodes are fragile and can easily break during implantation or during the experiment. Metal oxide microelectrodes are robust but they are prone to interference from redox species<sup>11</sup>, such as 3,4-dihydroxyacetic acid (DOPAC) and ascorbic acid that are present in the extracellular fluid<sup>12</sup>. Also, obtaining subsecond temporal resolution is difficult with these probes<sup>13</sup>. Other limitations of potentiometric measurements in general are their substantial drift, and their susceptibility to electronic noise. Indeed, environmental factors that alter the electrode potential can be mistakenly identified as a pH shifts<sup>14</sup>.

Fast-scan cyclic voltammetry (FSCV) with carbon-fiber microelectrodes was previously described as a method to measure pH in the brain *in vivo*<sup>5, 15, 16</sup>. The advantages of this approach to measuring local pH changes include the small probe size that leads to minimal tissue damage<sup>17</sup>, excellent spatial resolution, subsecond temporal resolution and the ability to use the sensor chronically<sup>18</sup>. Another distinguishing feature of FSCV detection of pH is the presence of a characteristic cyclic voltammogram (CV) for pH changes. The CV can be used as an electrochemical fingerprint for the qualitative identification of a pH signal, which can help to avoid any ambiguity associated with experimental artifacts that can be present using potentiometric measurements.

In addition to pH measurement, carbon-fiber microelectrodes coupled with FSCV are used for detection of catecholamines *in vitro* and *in vivo*<sup>19, 20</sup>. In previous studies *in vivo* shifts in pH were considered to be an interference for dopamine detection, and attempts were made to lessen the amplitude of this interference<sup>21</sup>. Since then, advancements in the field of *in vivo* voltammetry such as an increase in sensitivity towards dopamine<sup>22</sup>, the use of principal component regression for analysis of *in vivo* data<sup>23</sup> and the establishment of the physiological relevance of *in vivo* pH shifts after electrical stimulation<sup>5</sup> led to the realization that pH signals obtained with FSCV are valuable indicators of brain activity rather than an undesired artifact<sup>6, 15</sup>.

Cyclic voltammetry provides the opportunity to qualitatively identify an analyte through its electrochemical signature (i.e. cyclic voltammogram)<sup>24, 25</sup>. The identification of peaks can be difficult, however, when multiple physical processes take place simultaneously. Understanding the electrochemical processes responsible for the shape of the background-subtracted cyclic voltammogram relating to pH changes is crucial for appropriate interpretation of *in vivo* electrochemical data because of the opportunities for chemical interference in the brain.

The fast scan rates used with *in vivo* cyclic voltammetry result in a substantial background current due to charging of the electrode double layer and redox reactions of electrochemically active surface groups<sup>21</sup>. The background current remains constant for time periods less than 90 sec, so it can be digitally subtracted from the cyclic voltammogram when recorded in the presence of the electrochemically active species.

Peaks in the background subtracted cyclic voltammogram in response to a pH change are caused by a shift in the background of carbon electrode. The shape and magnitude of the background shift are defined by the electrochemically active surface groups present on the electrode surface. Surface oxide groups such as phenols, ortho- and para-quinones, carbonyls, lactones and carboxylic acids are reported to be found on carbon surface<sup>26</sup>. All of these groups are either susceptible to protonation-deprotonation or electrochemical oxidation/reduction reactions involving protons. The first comprehensive analytical method for quantifying of these groups on carbon electrode surface were developed in the 1960s in the form of a Boehm titration<sup>27</sup>, and were subsequently improved by modern instrumental physical methods for characterization of carbon surface<sup>28</sup>. However, neither of these methods can be used *in situ* to establish a connection between specific types of active surface groups with peaks observed in the cyclic voltammogram during an electrochemical experiment.

Despite the aforementioned advantages of *in vivo* pH detection using FSCV, the electrochemistry behind the origins of its CV generation is poorly characterized. Furthermore, the shape of the CV recorded *in vivo* often differs from those recorded *in vitro*. This shortcoming casts doubt on the identity of electrochemical signal observed in the brain. In this work we characterized FSCV pH signal *in vitro* to establish possible inferences and to make sure that FSCV measurement of pH satisfies the criteria for *in vivo* biosensors previously suggested<sup>29</sup>.

## EXPERIMENTAL SECTION

### Chemicals

All chemicals were obtained from Sigma-Aldrich (St. Louis, MO, USA) unless otherwise noted and used as received. Solutions were prepared using doubly distilled deionized water. Electrochemical experiments were done in PBS buffer (140 mM NaCl, 3 mM KCl, 10 mM

NaH<sub>2</sub>PO<sub>4</sub>, pH 7.4). A stock solution of 10 mM DOPAC was prepared in 0.1 N HClO<sub>4</sub> and diluted to the desired concentration immediately before use with the working buffer.

### Fabrication of Carbon Fiber Microelectrodes

Cylindrical microelectrodes were constructed using a T-650 carbon fiber (Thornel, Amoco Corp., Greenville, SC, USA) as previously described<sup>30</sup>. Briefly, individual carbon fibers were aspirated into glass capillaries (A-M Systems, Carlsborg, WA, USA). Afterwards, the capillaries were pulled with a micropipette puller (Narishige, Tokyo, Japan). The carbon fibers extruding from the pulled tip were cut to length of ~ 100 μm under an optical microscope. Before electrochemical experiments, electrodes were soaked in isopropanol purified with Norit A activated carbon (ICN, Costa Mesa, CA, USA) for at least 20 min to remove surface impurities<sup>31</sup>. Electrical connection to the carbon fiber was made with an electrolytic solution (4 M CH<sub>3</sub>COOK and 0.15 M KCl), and a stainless steel wire.

### Electrochemical Experiments

Cyclic voltammograms were acquired with either an EI-400 potentiostat used in two electrode mode (for flow injection experiments) or UEI (UNC Department of Chemistry Electronic Shop) potentiostat (for *in vivo* experiments) and TH-1 software (ESA Inc, Chemsfold, MA, USA) written in LabVIEW (National Instruments, Austin, TX, USA). The waveform was generated and the voltammetric signal was acquired with a PCI-6251 ADC/DAC card (National Instruments). A PCI-6711 DAC board (National Instruments) was used to synchronize waveform application, data acquisition and TTL pulses for the flow injection valve. The output waveform was filtered with a low pass 2 kHz filter to eliminate digitization steps as previously described<sup>32</sup>. Some data are presented in form of color plots<sup>33</sup>.

A triangular waveform with potential limits ranging from -0.4 V to 1.3 V was used at a scan rate of 400 V s<sup>-1</sup> for all voltammetric measurements. This waveform was applied at 10 Hz with a rest potential of -0.4 V between scans. Prior to measurements, carbon-fiber microelectrodes were electrochemically pretreated with this waveform at frequency of 60 Hz for 15 minutes<sup>22</sup>. Potentials are reported versus an Ag/AgCl reference electrode. Electrochemical measurements were performed in a grounded Faraday cage.

All data was analyzed and plotted using TH-1 software, MS Excel (Microsoft Corporation, Redmond, WA) or GraphPad Prism (GraphPad Software, San Diego, CA, USA). All values are given as averages with sample standard deviation unless the otherwise stated.

### Flow Injection Apparatus

The flow-injection analysis system consisted of a syringe pump (Harvard Apparatus, Holliston, MA) that directed buffer solution through a Teflon tube to a 6-port injection valve (Rheodyne, Rohnert Park, CA, USA) at rate of 0.5 mL per minute as previously described<sup>34</sup>. The injection valve was controlled by a 12 V DC solenoid and was used to introduce analyte from an injection loop (volume of 0.7 mL) into an electrochemical cell. The carbon-fiber microelectrode was placed inside the opening of the Teflon tube to eliminate diffusional broadening and the reference electrode was placed within ~ 20 mm of the working electrode<sup>34</sup>.

### Animal Experimentation

*In vivo* experiments were conducted in male Sprague-Dawley rats (250–400 g), (Charles River Laboratories, Wilmington, MA). Rats were anesthetized with urethane (50% w/w saline solution, 3 ml/kg, i.p.) and mounted in a stereotaxic frame (Kopf instruments, Tujunga, CA) which included a mounted gas anesthesia mask (Parkland Scientific, Inc,

Coral Springs, FL). The animal was provided with compressed air (60 mbar) for breathing under normal conditions. Holes for electrodes were drilled in skull precisely in the regions of interest using stereotaxic coordinates (caudate-putamen: +1.2 mm anterior-posterior and +2.1 mm medial-lateral to bregma for hypercapnia experiments and nucleus accumbens: +2.2 mm anterior-posterior and +1.5 mm medial-lateral to study the effect of DOPAC on pH change cyclic voltammograms)<sup>35</sup>. The reference electrode (Ag/AgCl) was placed contralaterally to the working electrode. The bipolar stimulating electrode (Plastics One, Roanoke, VA, USA) was placed in the substantia nigra/ventral tegmental area (SN/VTA) (-5.6 mm anterior-posterior and +1.0 mm medial-lateral to bregma). TH-1 software was used to generate biphasic stimulation pulses (60 pulses, 60 Hz, 300  $\mu$ A, 2 ms per phase) which were sent to optically insulated, constant current stimulators (NeuroLog System, Hertfordshire, UK) and synchronized to occur between voltammetric scans.

The position of the working electrode (-4.5 mm dorsal-ventral from the skull surface) and the stimulating electrode (-7.5 mm dorsal-ventral from the skull surface) were optimized to maximize electrically evoked basic pH change<sup>5</sup>. Once the basic pH change after electrical stimulation was observed, hypercapnic states were induced by switching the breathing gas from compressed air to compressed carbon dioxide (also at 60 mbar) for brief period of time (5–10 seconds) and then switched back to air.

All animal protocols and care were approved by the Institutional Animal Care and Use Committee of the University of North Carolina at Chapel Hill.

## RESULTS AND DISCUSSION

### Characterization of the Peaks in Cyclic Voltammogram for pH change

Previous work using carbon microelectrodes has suggested that two of the peaks in the background subtracted cyclic voltammogram for a pH change are due to the background shift associated with the pH-dependent electrochemical oxidation of a hydroquinone moiety on the carbon surface<sup>21, 36–38</sup>:



where  $\text{QH}_{2s}$  and  $\text{Q}_s$  denote the reduced and oxidized form of a surface bond hydroquinone-like moiety whose structure is unknown. There are two peaks (Figure 1A) in the background subtracted cyclic voltammogram for acidic pH shift that correspond to this electrochemical reaction. Here, these peaks are denoted as a QH-peak (for the hydroquinone to quinone transition occurring at approximately 0.3 V on the positive sweep at a pH of 7.4) and a Q-peak (for the quinone to hydroquinone transition occurring at approximately -0.3 V on the negative sweep at a pH of 7.4). There are several pieces of evidence in support of this hypothesis. Recently, it was demonstrated that hydroxide groups exist on carbon-fiber microelectrodes when used in similar FSCV experiments<sup>39</sup>. Also, carbon electrodes that were purposefully modified with hydroquinone moiety show the same hydroquinone oxidation-reduction peaks on cyclic voltammograms as peaks in the background of electrochemically oxidized carbon-fiber microelectrodes<sup>16, 40</sup>. Furthermore, the QH-peak in the background current is located at the same potential (~0.09V, Figure 2C) as oxidation peak of surface immobilized hydroquinone moiety<sup>16</sup>. Moreover, the QH-peak shifts with pH in a similar way as it was previously reported<sup>21</sup>.

In addition to these two hydroquinone peaks, there is a third peak at potential of -0.2 V on the anodic sweep that denoted here as the C-peak (Figure 1A and B). A background subtracted cyclic voltammogram for basic pH shift (Figure 1B) implies that increase in pH

decreases capacitance (C-peak) and also causes a shift of QH- and Q-peaks of the background current. The nature of the C-peak was investigated further in this work.

The advantage of using FSCV on carbon-fiber microelectrodes for the detection of pH changes is the signature voltammogram (Figure 1A and B) that enables qualitative identification of pH shifts. Since fast-scan cyclic voltammetry is differential technique, typically only background subtracted cyclic voltammograms are used for data representation. In a background subtracted cyclic voltammogram each peak has two possible origins. Oxidation of analyte at certain potential produces a peak after subtraction in the same fashion as it is in traditional cyclic voltammogram. Besides this, shift in position of the peaks in background produces peaks in background subtracted cyclic voltammograms. In case of pH changes both of these events might take place. Because of this, the amplitude of current for characteristic peaks in background subtracted cyclic voltammogram is used for calibration and not the peak potential as it was suggested elsewhere<sup>16</sup>.

The magnitude of the current for each of the peaks varies linearly with pH shifts within physiological pH range from 7.2 to 7.6. The slopes for the calibration curves are  $-52 \pm 2$  nA/pH for the C-peak,  $-42 \pm 1$  nA/pH for the Q-peak and  $-110 \pm 2$  nA/pH for the QH-peak ( $n = 3$ ).  $R^2$  values of the linear fit are 0.95, 0.97 and 0.99 for C-peak, HQ-peak and Q-peak respectively.

### Capacitive Contributions to the Cyclic Voltammogram for pH change

The potentials where oxidation and reduction occur for an electrochemical reaction are a function of the propensity of a species to give and receive electrons, electron-transfer kinetics and analyte mass-transport. For these reasons electrochemical peaks in cyclic voltammograms related to a specific faradaic redox processes are generally located at well-defined positions. In contrast, the nonfaradaic process of the charging of the double layer produces peaks which are potential independent, and are instead defined by the time constant (RC) of the electrode given that the capacitance of the double layer does not change appreciably in a certain potential window<sup>24</sup>. The potential dependency of peaks, therefore, can be used to distinguish between faradaic and nonfaradaic processes.

To distinguish whether the observed peaks were faradaic or nonfaradaic processes, the initial potential was applied at three different values ( $-0.4$  V to  $-0.5$  and  $-0.6$  V). The position of the QH- and Q-peaks remained consistent for both acidic (Figure 2A) and basic (Figure 2B) pH shifts with all three initial potentials, confirming that these peaks have faradaic origin. On the contrary, the C-peak in a pH cyclic voltammogram shifted 0.1 V and 0.2 V relative to that with an initial potential of  $-0.4$  V for the  $-0.5$  and  $-0.6$  V potential limits respectively. This potential dependence indicates that the C-peak results from a change in a nonfaradaic process related to charging of the double layer. In the background cyclic voltammogram from which the pH changes were extracted, the potential of the C-peak coincides with a current deflection that occurs around  $-0.2$  V (Figure 2C) with initial potential of  $-0.4$  V. This deflection was also shifted 0.1 V and 0.2 V for the  $-0.5$  and  $-0.6$  V potential expansions, respectively (Figure 2C). This current deflection has been previously attributed to double layer charging<sup>22</sup> and our current work clearly illustrates the validity of this assignment. This result establishes a link between a change in pH and its effect on the double layer capacitance. Specifically a change in pH leads to a shift of the background current, which leads to the appearance of this peak upon background subtraction. As this peak arises from non-faradaic processes and not a chemical reaction, it will be referred as the C-peak throughout the rest of this manuscript.



## Background-subtracted Cyclic Voltammograms due to the Adsorption of Electrochemically Inert Species

Background-subtracted FSCV at carbon-fiber microelectrodes was developed as a technique for detection of electrochemically active biogenic amines<sup>19</sup>, primarily dopamine. The electrochemical conditions used for FSCV were optimized to increase sensitivity towards catecholamines. The adsorption of catecholamines to the carbon-fiber surface is mainly responsible for the low limits of detection (tens of nM) reached by FSCV<sup>22</sup>. At physiological concentrations of dopamine, adsorbed molecules account for up to 95% of the electrochemical current while only 5% results from molecules that diffuse towards the microelectrode during the potential sweep<sup>31, 41</sup>. Catecholamine adsorption is generally achieved by holding the microelectrode for 100 milliseconds (for 10 Hz frequency) at a negative potential (−0.4 V) between voltammetric sweeps. This leads to amplification of catecholamine adsorption due to electrostatic interaction<sup>22</sup> between positively charged dopamine molecules and the carbon surface. However, holding at a negative potential additionally promotes the adsorption of other species, especially those that are positively charged and those containing aromatic moieties. The contribution of adsorption to the FSCV procedure was demonstrated previously<sup>31</sup>; however the effect of the adsorption with respect to pH measurements was not studied.

The adsorption of organic molecules to the electrode surface will affect the charging of the double layer by changing the double-layer capacitance. Therefore, the adsorption of these species will produce background-subtracted cyclic voltammograms that can be thought of as additive to any faradaic electrochemistry that occurs<sup>24, 25, 31</sup>. Generally, adsorption of neutral species on the uncharged surface causes a decrease in double layer capacitance since it displaces ions in the double layer further away from the electrode. If the adsorbing species is charged, the surface has charged groups, or electrode is held at some non-zero potential then the prediction of direction of the change in double-layer capacitance becomes more complex. Detailed quantitative description of the change in interfacial capacitance of a carbon electrode associated with adsorption is difficult because the nature and amount of active groups is unknown. Furthermore, as suggested in our previous work<sup>42</sup>, the composition of the carbon surface is not static but dynamically changes and depends on parameters of the electrochemical experiment (i.e. anodic potential limit). Previously, we suggested the existence of carboxylic groups on the surface of carbon-fiber microelectrode when higher anodic potential limits are used<sup>42</sup>. Here we investigate the adsorption of various species onto the carbon surface to test this hypothesis.

$\beta$ -phenylethylamine (PEA) at pH 7.4 is an electrochemically inert, positively charged, aromatic amine and has high affinity to carbon microelectrodes held at negative potentials<sup>31</sup>. When exposed to the carbon-fiber surface, it adsorbs, decreasing the double layer capacitance in a potential dependent fashion. This process results in a background-subtracted cyclic voltammogram with noticeable peaks (Figure 3A). If the decrease in double layer capacitance is potential independent then it should lead to a square-like cyclic voltammogram resulting due to altering the RC constant of the electrochemical cell. However, the background subtracted cyclic voltammograms related to PEA adsorption have a well pronounced negative peak. This shape indicates desorption of PEA induced by electrostatic repulsion when the potential of the electrode goes into the positive region.

Higher concentrations of PEA led to an increase in the amount of adsorbed molecules causing a measureable change in the background current. An adsorption isotherm that relates negative charge from the cyclic voltammogram to PEA concentration can be constructed (Figure 3D). The charge, which is proportional to surface coverage, does not reach saturation in the concentration range evaluated. This lack of saturation indicates that the

adsorption mechanism is not Langmuiric, but can be described rather by a Freundlich isotherm:

$$Q = \alpha C^\gamma \quad (2)$$

where Q is charge, C is concentration and  $\alpha$  and  $\gamma$  are empirical parameters. The Freundlich isotherm generally describes an adsorption process at a surface with heterogeneous adsorption sites<sup>43</sup>. Such is the case for carbon surfaces, as it was reported in earlier studies of electroadsorption of organic molecules on carbon-fibers<sup>44</sup>.

The tendency of electrochemically inert organic molecules to adsorb to carbon-fiber microelectrodes was previously reported for several drugs including nomifensine and GBR-12909 (dopamine transporter blockers)<sup>45</sup>. Both of these molecules are hydrophobic, positively charged, aromatic amines at physiological pH and apparently these properties strengthen their affinity for carbon surfaces. The fact that the presence of these molecules reduces FSCV sensitivity towards dopamine suggests that they compete for the same adsorption sites as catecholamines on carbon surfaces or, which is also possible, adsorption of these molecules renders the carbon surface hydrophobic and, hence, less wettable which in turn reduces dopamine adsorption.

Interestingly, adsorption of phenylacetic acid (PAA) leads to an increase in background current which is observed as a positive peak after the background subtraction (Figure 3C). At pH 7.4 PAA is a negatively charged aromatic species that is electrochemically inert. The increase in the background current can be explained by the fact that adsorption of PAA brings additional negative charge to the electrode surface which in turn shifts the electrode potential further from the potential of zero charge and attracts more positively charged counter ions. This potential shift, therefore, leads to an increase in double layer capacitance.

However, organic aromatic molecules are not the only species that have affinity to the carbon electrode surface. Positively charged calcium ions also can adsorb to a carbon surface. This again results in a change of the background current and a cyclic voltammogram with negative peak (Figure 3B). Adsorption isotherms of  $\text{Ca}^{2+}$  constructed for a range of concentrations from 5 to 500  $\mu\text{M}$  also implies a Freundlich adsorption mechanism (Figure 3E). The endogenous concentration of  $\text{Ca}^{2+}$  in the extracellular fluid is 1–2 mM and it is tightly regulated<sup>46</sup>. This concentration corresponds to the relatively flat part of the isotherm which means that moderate changes in calcium concentration should not affect the microelectrode sensitivity towards pH shifts or catecholamine detection.

Previously, it was shown that both  $\text{Ca}^{2+}$  and  $\text{Mg}^{2+}$  ions reduce FSCV sensitivity to dopamine<sup>47, 48</sup>; this again suggests that these ions adsorb to the same adsorption sites as dopamine. The surface-bound carboxylic groups might be of critical importance to this adsorption process<sup>42</sup>. Alkali-earth metals have a strong tendency to form complexes with ligands that have carboxylic groups such as EDTA<sup>49</sup>. We hypothesize that the formation of such complexes with carboxylic groups on carbon surface is also possible. In fact, barium ions binding to surface bound carboxylic and hydroxylic groups on carbon was used as a labeling technique to quantify the amount of these groups with X-ray photoelectron spectroscopy (XPS)<sup>50</sup>; therefore, the formation of these complexes with calcium is a viable possibility. Also, it was shown that calcium ions can strongly adsorb to surface immobilized carboxylic groups and completely eliminate the voltammetric peak related to protonation-deprotonation of these carboxylic groups<sup>51</sup>. Indirect confirmation of the carboxylic-group hypothesis may be given if the presence of calcium leads to the suppression of the C-peak in the background charging current.



## Distortion of Cyclic Voltammograms for pH change due to Adsorption of Electrochemically Inert Species

The experimental data presented here implies that alteration of the double layer induced by protonation/deprotonation of the electrode surface causes the C-peak in the pH change cyclic voltammogram. Since other chemical species are present that can perturb the electrode double layer, it is logical to propose that the presence of these species in solution may alter the shape of the pH change cyclic voltammogram. This interference does not abolish the sensitivity to the pH changes, but distorts the shape of the cyclic voltammogram which can make it difficult to identify the signal for pH change.

The distortion of the pH change cyclic voltammogram in the presence of adsorbing species was investigated to provide a qualitative relationship between *in vivo* and *in vitro* data. PEA at a concentration of 500  $\mu\text{M}$  decreases the amplitude of the C-, QH- and Q-peaks (Figure 4A). Also, it changes the relative height of C-peak compared to the QH-peak. Normally, the amplitude of the C-peak is larger than QH-peak, but the addition of PEA decreased the amplitude of the C-peak to greater extent than the QH-peak, making the amplitudes of both peaks approximately equal. Calcium at a concentration of 500  $\mu\text{M}$  has a similar effect on the cyclic voltammogram in addition to a more pronounced effect on the amplitude of the Q-peak (Figure 4B).

The addition of tris(hydroxymethyl)aminomethane (TRIS) at 15 mM also decreased the amplitude of all three peaks with the dramatic suppression in C-peak (Figure 4C). Traditionally, TRIS based buffer has been used for post *in vivo* calibration of carbon-fiber microelectrodes, but inconsistencies existed between the cyclic voltammograms obtained for pH shifts measured *in vitro* using TRIS buffer and those obtained through *in vivo* experiments. The use of TRIS buffer is therefore not advised for pH calibration since it distorts both the shape and amplitude of the response to pH changes.

The data suggest adsorptive species might interfere with detection of pH changes using FSCV with carbon-fiber microelectrodes. Brain extracellular fluid contains small organic molecules including amino acids and proteins which can adsorb to the carbon surface<sup>52</sup>. Nevertheless, successful use of FSCV for detection of pH shifts in dopaminergic brain regions for several years proves that this interference is minimal<sup>5, 6, 15</sup>. Furthermore, the recent discovery the carbon electrode surface regeneration occurs when the potential is scanned to 1.3V<sup>42</sup> assures that long term deterioration of the carbon electrode surface is minimized.

We recommend the use of QH-peak for pH detection. The amplitude of the C-peak is sensitive to adsorption. The Q-peak is unsatisfactory because it can be pushed to more negative potentials so it is not completely within the potential window of the cyclic voltammogram.

## Distortion of Cyclic Voltammogram for pH change from DOPAC

Changes in pH should cause a shift in the electrochemical peaks that originate from all electrochemical reactions that involve either protons or hydroxides<sup>38</sup>. The shift in the redox peaks of surface bound hydroquinone moieties causes the appearance of QH- and Q-peaks in cyclic voltammogram for a pH change. Besides surface bound electroactive groups, there are many electrochemically active species in the extracellular fluid of the rat striatum which may participate in redox reactions involving protons. The most abundant are ascorbic acid, uric acid, homovanillic acid and DOPAC<sup>53</sup>. Any of these species can potentially interfere with pH detection since they have proton-dependent electrochemistry.

DOPAC is a major metabolite of dopamine that has similar electrochemical properties. In addition, DOPAC is the catechol that is present in the brain in highest concentration. The concentration of DOPAC in rat striatum is about 20–30  $\mu\text{M}$ <sup>12, 54</sup> compared to about 20 nM for dopamine<sup>55</sup>. Also, FSCV is ten times more sensitive to dopamine than DOPAC<sup>56</sup>; it is not enough to account for the one thousand difference in concentration between DOPAC and dopamine. This makes DOPAC a likely cause of distortion for pH cyclic voltammogram.

Since DOPAC is a catechol, it follows the same oxidation reaction pathway as other catechols (Equation 1). Thus, an acidic pH shift should shift the cyclic voltammogram for DOPAC to more positive potentials. In the background subtracted voltammogram this will result in two additional peaks on the cyclic voltammogram for a pH shift. *In vitro* experiments confirm this hypothesis. Figure 5 shows cyclic voltammograms of DOPAC in PBS buffer and shows the appearance of additional peaks at  $\sim 0.6$  V on the anodic scan and  $\sim -0.2$  V on the cathodic scan for acidic pH shift (Figure 5A). Peaks at the same potentials are also present for a basic pH shift (Figure 5B). These extra peaks are visible in cyclic voltammograms for electrically evoked pH change *in vivo*. As expected, some *in vivo* cyclic voltammograms indeed have these peaks (Figure 5C). The anodic peak was well pronounced and located at the same potential as it was *in vitro* (compare to Figure 5B) while the cathodic peak is merged together with QH-peak.

Ascorbic acid can be an interferent, but it has slow electron transfer and irreversible electrochemistry at given conditions<sup>22</sup>. It is unlikely that ascorbic acid is responsible for distortion of *in vivo* cyclic voltammogram for pH change since that distortion it features two peaks. Also, uric acid can potentially interfere, but we suspect that its extracellular concentration in rat striatum is small since tissue damage is minimal with carbon-fiber microelectrode<sup>57</sup>. In turn, homovanillic acid has quasi-reversible electrochemistry and can produce two peaks. However, position of peak from interference at  $\sim 0.6$  V in cyclic voltammogram recorded *in vivo* makes homovanillic acid improbable candidate because at given conditions it oxidizes at  $\sim 0.8\text{V}$ <sup>22</sup>, thus in case of interference the peak would be at  $\sim 0.8\text{V}$  as well.

This distortion induced by DOPAC was not previously reported, however it is critical for qualitative identification of pH signal *in vivo*. Although DOPAC is generally absent in the post-calibration buffer, its addition should be considered to better mimic the *in vivo* environment.

### Verification of FSCV pH Signal with Acidosis Induced by Hypercapnia

According to previously suggested criteria for the validation of signals from an *in vivo* biosensor, physiological relevance of the obtained data should be established<sup>29</sup>. In case of *in vivo* pH sensor, transiently induced pH shift in the brain is required. The shift should be well controlled and the physiological mechanism behind this pH change should be well understood. These requirements are necessary for establishing confidence that the pH is actual chemical species that are measured with the sensor.

Electrical stimulation of neurons is widely used in study of neuronal transmission. In our previous work we showed that electrical stimulation of dopaminergic neurons can be used to induce transient pH change<sup>5</sup>. However, before pH changes induced by electrical stimulation were detected with FSCV, it was not obvious that such stimulation of dopamine neurons should cause basic pH changes.

In this work the concentration of carbon dioxide in inhaled air was altered to produce hypercapnia and induce acidosis. Hypercapnia is a physiological effect caused by an

increase in carbon dioxide in the blood and it is well known to produce transient pH changes in the brain<sup>3, 58–60</sup>. In hypercapnia experiment, the breathing mixture for the anesthetized animal was transiently changed from air to carbon dioxide for a 5 second interval. All of the data cyclic voltammograms recorded in the 30 seconds interval around carbon dioxide inhalation are shown in the form of a color plot where the ordinate is the applied potential and the abscissa is time with current encoded in false color<sup>33</sup> (Figure 6A). A representative cyclic voltammogram obtained during acidosis (20 sec after application of carbon dioxide) contains all of the characteristic peaks as an acidic pH cyclic voltammogram acquired *in vitro* (compare Figure 6B with Figure 2B). Besides C-, QH- and Q-peak it also has a DOPAC related peak at potential of ~ 0.7 V on anodic scan. Current traces at a potential of +0.15 V (QH-peak) shows monophasic drop in pH calculated to be 0.05 pH units (Figure 6C). Previous studies of hypercapnia in similar conditions using glass pH microelectrode had much slower time resolution (5 minutes). The drop in pH of ~ 0.8 units was observed in first 5 minutes after application of carbon dioxide<sup>58</sup>. Since time resolution of FSCV is much better and only first 20 seconds of hypercapnia was investigated, it is reasonable to observe smaller drop in pH.

## CONCLUSIONS

Background subtracted fast-scan cyclic voltammetry with carbon-fiber microelectrodes can be used as a reliable method for the detection of transient pH changes in intact brain tissue *in vivo*. The presence of the signature cyclic voltammogram for pH is an excellent qualitative indicator that allows for the selective identification of proton concentration change over fluctuations associated with other chemical species. However, interference from electrochemically inert species, and from electrochemically active species with proton-dependent electrochemistry, can distort the shape of the cyclic voltammogram for pH shifts. This distortion should be taken in consideration both for *in vivo* experiments and *in vitro* calibration of carbon-fiber microelectrodes to maintain selectivity for pH measurements. Acidosis induced by hypercapnia was used as a convenient method to change in pH in the brain. Comparing the cyclic voltammograms recorded with this pH sensor *in vitro* with voltammograms obtained during transient physiological pH changes *in vivo* induced by hypercapnia was used as a verification that the signals obtained from the sensor is actually pH changes.

However, there are several limitations of FSCV with respect to pH measurements. FSCV is only good for differential measurements, so absolute value of pH cannot be established. Also, only measurements on short time scale of no more than 120 seconds are possible due to drift of the electrode background. In some cases this limitation can be fixed using analog background subtraction technique<sup>61</sup>. Furthermore, glass-encased carbon microelectrodes are fragile and, probably, less robust than microfabricated potentiometric IrOx probes<sup>10</sup>. However, the silica encased carbon fibers used chronically<sup>18</sup> and recently developed pyrolyzed photoresist carbon arrays for *in vivo* applications<sup>62</sup> are much more robust and hopefully replace the fragile glass microelectrodes in the future.

## Acknowledgments

The authors acknowledge financial support from NIH (NS 15841), Eli Lilly Fellowship for P.T., NIH (DA023586) to G.S.M. R.B.K. is supported by a National Defense Science & Engineering Graduate Fellowship.

## References

1. Heisler, N. Acid-base regulation in animals. Elsevier; Amsterdam; New York; New York, NY, U.S.A: 1986.
2. Kaila, K.; Ransom, BR. pH and brain function. Wiley-Liss; New York: 1998. p. xiiip. 688

3. Siesjo BK. Regulation of Cerebrospinal-Fluid pH. *Kidney International* 1972;1 (5):360–374. [PubMed: 4599953]
4. Chesler M. Regulation and modulation of pH in the brain. *Physiological Reviews* 2003;83 (4):1183–1221. [PubMed: 14506304]
5. Venton BJ, Michael DJ, Wightman RM. Correlation of local changes in extracellular oxygen and pH that accompany dopaminergic terminal activity in the rat caudate-putamen. *Journal of Neurochemistry* 2003;84 (2):373–381. [PubMed: 12558999]
6. Roitman MF, Wheeler RA, Wightman RM, Carelli RM. Real-time chemical responses in the nucleus accumbens differentiate rewarding and aversive stimuli. *Nature Neuroscience* 2008;11 (12):1376–1377.
7. Ziemann AE, Allen JE, Dahdaleh NS, Drebot II, Coryell MW, Wunsch AM, Lynch CM, Faraci FM, Howard MA, Welsh MJ, Wemmie JA. The Amygdala Is a Chemosensor that Detects Carbon Dioxide and Acidosis to Elicit Fear Behavior. *Cell* 2009;139 (5):1012–1021. [PubMed: 19945383]
8. Korostynska O, Arshak K, Gill E, Arshak A. Review paper: Materials and techniques for in vivo pH monitoring. *Ieee Sensors Journal* 2008;8 (1–2):20–28.
9. Fedirko N, Svichar N, Chesler M. Fabrication and use of high-speed, concentric H<sup>+</sup>- and Ca<sup>2+</sup>-selective microelectrodes suitable for in vitro extracellular recording. *Journal of Neurophysiology* 2006;96 (2):919–924. [PubMed: 16672303]
10. Johnson MD, Kao OE, Kipke DR. Spatiotemporal pH dynamics following insertion of neural microelectrode arrays. *Journal of Neuroscience Methods* 2007;160 (2):276–287. [PubMed: 17084461]
11. Fog A, Buck RP. Electronic Semiconducting Oxides as pH Sensors. *Sensors and Actuators* 1984;5 (2):137–146.
12. Bassetomusk A, Rebec GV. Regional Distribution of Ascorbate and 3,4-Dihydroxyphenylacetic Acid (Dopac) in Rat Striatum. *Brain Research* 1991;538 (1):29–35. [PubMed: 2018931]
13. Kinlen PJ, Heider JE, Hubbard DE. A Solid-State pH Sensor-Based on a Nafion-Coated Iridium Oxide Indicator Electrode and a Polymer-Based Silver-Chloride Reference Electrode. *Sensors and Actuators B-Chemical* 1994;22 (1):13–25.
14. Galster, H. pH measurement: fundamentals, methods, applications, instrumentation. VCH; Weinheim, Federal Republic of Germany; New York, NY, USA: 1991. p. xviii. 356
15. Cheer JF, Wassum KM, Wightman RM. Cannabinoid modulation of electrically evoked pH and oxygen transients in the nucleus accumbens of awake rats. *Journal of Neurochemistry* 2006;97 (4):1145–1154. [PubMed: 16686693]
16. Makos MA, Omiattek DM, Ewing AG, Heien ML. Development and Characterization of a Voltammetric Carbon-Fiber Microelectrode pH Sensor. *Langmuir* 2010;26 (12):10386–10391. [PubMed: 20380393]
17. Jaquins-Gerstl A, Michael AC. Comparison of the brain penetration injury associated with microdialysis and voltammetry. *Journal of Neuroscience Methods* 2009;183 (2):127–135. [PubMed: 19559724]
18. Clark JJ, Sandberg SG, Wanat MJ, Gan JO, Horne EA, Hart AS, Akers CA, Parker JG, Willuhn I, Martinez V, Evans SB, Stella N, Phillips PEM. Chronic microsensors for longitudinal, subsecond dopamine detection in behaving animals. *Nat Meth* 2009;7 (2):126–129.
19. Robinson DL, Hermans A, Seipel AT, Wightman RM. Monitoring rapid chemical communication in the brain. *Chemical Reviews* 2008;108 (7):2554–2584. [PubMed: 18576692]
20. Kita JM, Wightman RM. Microelectrodes for studying neurobiology. *Current Opinion in Chemical Biology* 2008;12 (5):491–496. [PubMed: 18675377]
21. Runnels PL, Joseph JD, Logman MJ, Wightman RM. Effect of pH and surface functionalities on the cyclic voltammetric responses of carbon-fiber microelectrodes. *Analytical Chemistry* 1999;71 (14):2782–2789. [PubMed: 10424168]
22. Heien MLAV, Phillips PEM, Stuber GD, Seipel AT, Wightman RM. Overoxidation of carbon-fiber microelectrodes enhances dopamine adsorption and increases sensitivity. *Analyst* 2003;128 (12):1413–1419. [PubMed: 14737224]
23. Heien MLAV, Khan AS, Ariansen JL, Cheer JF, Phillips PEM, Wassum KM, Wightman RM. Real-time measurement of dopamine fluctuations after cocaine in the brain of behaving rats.

- Proceedings of the National Academy of Sciences of the United States of America 2005;102 (29): 10023–10028. [PubMed: 16006505]
24. Bard, AJ.; Faulkner, LR. *Electrochemical Methods*. Wiley; New York: 2001.
  25. Kissinger, PT.; Heineman, WR. *Laboratory Techniques in Electroanalytical Chemistry*. Marcel Dekker Inc; 1996.
  26. McCreery RL. Advanced carbon electrode materials for molecular electrochemistry. *Chemical Reviews* 2008;108 (7):2646–2687. [PubMed: 18557655]
  27. Boehm HP, Heck W, Sappok R, Diehl E. *Surface Oxides of Carbon*. *Angewandte Chemie-International Edition* 1964;3(10):669.
  28. Boehm HP. Surface oxides on carbon and their analysis: a critical assessment. *Carbon* 2002;40 (2): 145–149.
  29. Phillips PEM, Wightman RM. Critical guidelines for validation of the selectivity of in-vivo chemical microsensors. *Trac-Trends in Analytical Chemistry* 2003;22 (9):509–514.
  30. Cahill PS, Walker QD, Finnegan JM, Mickelson GE, Travis ER, Wightman RM. Microelectrodes for the measurement of catecholamines in biological systems. *Analytical Chemistry* 1996;68 (18): 3180–3186. [PubMed: 8797378]
  31. Bath BD, Michael DJ, Trafton BJ, Joseph JD, Runnels PL, Wightman RM. Subsecond adsorption and desorption of dopamine at carbon-fiber microelectrodes. *Analytical Chemistry* 2000;72 (24): 5994–6002. [PubMed: 11140768]
  32. Zachek MK, Takmakov P, Moody B, Wightman RM, McCarty GS. Simultaneous Decoupled Detection of Dopamine and Oxygen Using Pyrolyzed Carbon Microarrays and Fast-Scan Cyclic Voltammetry. *Analytical Chemistry* 2009;81 (15):6258–6265. [PubMed: 19552423]
  33. Michael DJ, Joseph JD, Kilpatrick MR, Travis ER, Wightman RM. Improving data acquisition for fast scan cyclic voltammetry. *Analytical Chemistry* 1999;71 (18):3941–3947. [PubMed: 10500480]
  34. Kristensen EW, Wilson RL, Wightman RM. Dispersion in Flow-Injection Analysis Measured with Microvoltammetric Electrodes. *Analytical Chemistry* 1986;58 (4):986–988.
  35. Paxinos, G.; Watson, C. *The rat brain in stereotaxic coordinates*. Academic Press/Elsevier; Amsterdam; Boston: 2007.
  36. Elliott CM, Murray RW. *Chemically Modified Carbon Electrodes*. *Analytical Chemistry* 1976;48 (8):1247–1254.
  37. Evans JF, Kuwana T. Introduction of Functional-Groups onto Carbon Electrodes Via Treatment with Radio-Frequency Plasmas. *Analytical Chemistry* 1979;51 (3):358–365.
  38. Kawagoe KT, Garris PA, Wightman RM. pH-Dependent Processes at Nafion(R)-Coated Carbon-Fiber Microelectrodes. *Journal of Electroanalytical Chemistry* 1993;359 (1–2):193–207.
  39. Roberts JG, Moody BP, McCarty GS, Sombers LA. Specific Oxygen-Containing Functional Groups on the Carbon Surface Underlie an Enhanced Sensitivity to Dopamine at Electrochemically Pretreated Carbon Fiber Microelectrodes. *Langmuir* 2010;26 (11):9116–9122. [PubMed: 20166750]
  40. Aklilu M, Tessema M, Redi-Abshiro M. Indirect voltammetric determination of caffeine content in coffee using 1,4-benzoquinone modified carbon paste electrode. *Talanta* 2008;76 (4):742–746. [PubMed: 18656651]
  41. Baur JE, Kristensen EW, May LJ, Wiedemann DJ, Wightman RM. Fast-Scan Voltammetry of Biogenic Amines. *Analytical Chemistry* 1988;60 (13):1268–1272. [PubMed: 3213946]
  42. Takmakov P, Zachek MK, Keithley RB, Walsh PL, Donley C, McCarty GS, Wightman RM. Carbon Microelectrodes with a Renewable Surface. *Analytical Chemistry* 2010;82 (5):2020–2028. [PubMed: 20146453]
  43. Tóth, J. *Adsorption: theory, modeling, and analysis*. Marcel Dekker; New York: 2002. p. viii. 878
  44. Woodard FE, McMackins DE, Jansson REW. Electrosorption of Organics on 3-Dimensional Carbon-Fiber Electrodes. *Journal of Electroanalytical Chemistry* 1986;214 (1–2):303–330.
  45. Davidson C, Ellinwood EH, Douglas SB, Lee TH. Effect of cocaine, nomifensine, GBR 12909 and WIN 35428 on carbon fiber microelectrode sensitivity for voltammetric recording of dopamine. *Journal of Neuroscience Methods* 2000;101 (1):75–83. [PubMed: 10967364]

46. Somjen, GG. *Ions in the brain: normal function, seizures, and stroke*. Oxford University Press; Oxford; New York: 2004. p. xxixp. 470
47. Kume-Kick J, Rice ME. Dependence of dopamine calibration factors on media  $\text{Ca}^{2+}$  and  $\text{Mg}^{2+}$  at carbon-fiber microelectrodes used with fast-scan cyclic voltammetry. *Journal of Neuroscience Methods* 1998;84 (1–2):55–62. [PubMed: 9821634]
48. Chen BT, Rice ME. Calibration factors for cationic and anionic neurochemicals at carbon-fiber microelectrodes are oppositely affected by the presence of  $\text{Ca}^{2+}$  and  $\text{Mg}^{2+}$  *Electroanalysis* 1999;11 (5):344–348.
49. Bell, CF. *Principles and applications of metal chelation*. Clarendon Press; Oxford: 1977.
50. Denison P, Jones FR, Watts JF. X-Ray Photoelectron Spectroscopic Analysis of Barium-Labeled Carbon-Fiber Surfaces. *Journal of Materials Science* 1985;20 (12):4647–4656.
51. Rosendahl SM, Burgess IJ. Electrochemical and infrared spectroscopy studies of 4-mercaptobenzoic acid SAMS on gold surfaces. *Electrochimica Acta* 2008;53 (23):6759–6767.
52. Abe I, Hayashi K, Kitagawa M. The Adsorption of Amino-Acids from Water on Activated Carbons. *Bulletin of the Chemical Society of Japan* 1982;55 (3):687–689.
53. Justice, JB. *Voltammetry in the Neurosciences: Principles, Methods, and Applications*. Humana Press; Clifton, NJ: 1987.
54. Gonon F, Buda M, Cespuglio R, Jouvet M, Pujol JF. Voltammetry in the Striatum of Chronic Freely Moving Rats - Detection of Catechols and Ascorbic-Acid. *Brain Research* 1981;223 (1): 69–80. [PubMed: 7284811]
55. Shou MS, Ferrario CR, Schultz KN, Robinson TE, Kennedy RT. Monitoring dopamine in vivo by microdialysis sampling and on-line CE-laser-induced fluorescence. *Analytical Chemistry* 2006;78 (19):6717–6725. [PubMed: 17007489]
56. Heien MLAV, Johnson MA, Wightman RM. Resolving neurotransmitters detected by fast-scan cyclic voltammetry. *Analytical Chemistry* 2004;76 (19):5697–5704. [PubMed: 15456288]
57. Duff A, Oneill RD. Effect of Probe Size on the Concentration of Brain Extracellular Uric-Acid Monitored with Carbon-Paste Electrodes. *Journal of Neurochemistry* 1994;62 (4):1496–1502. [PubMed: 7510782]
58. Katsura K, Kristian T, Nair R, Siesjo BK. Regulation of Intracellular and Extracellular pH in the Rat-Brain in Acute Hypercapnia - a Reappraisal. *Brain Research* 1994;651 (1–2):47–56. [PubMed: 7922589]
59. Brian JE. Carbon dioxide and the cerebral circulation. *Anesthesiology* 1998;88 (5):1365–1386. [PubMed: 9605698]
60. Kintner DB, Anderson ME, Sailor KA, Diemel G, Fitzpatrick JH, Gilboe DD. In vivo microdialysis of 2-deoxyglucose 6-phosphate into brain: A novel method for the measurement of interstitial pH using P-31-NMR. *Journal of Neurochemistry* 1999;72 (1):405–412. [PubMed: 9886094]
61. Hermans A, Keithley RB, Kita JM, Sombers LA, Wightman RM. Dopamine detection with fast-scan cyclic voltammetry used with analog background subtraction. *Analytical Chemistry* 2008;80 (11):4040–4048. [PubMed: 18433146]
62. Zachek MK, Park J, Takmakov P, Wightman RM, McCarty GS. Microfabricated FSCV-compatible microelectrode array for real-time monitoring of heterogeneous dopamine release. *Analyst* 2010;135 (7):1556–1563. [PubMed: 20464031]



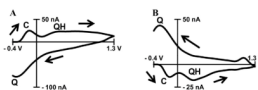


**Figure 1. Background subtracted cyclic voltammograms of pH shifts**

Identification of peaks in background-subtracted cyclic voltammograms for acidic ( $-0.25$  pH units, A) and basic ( $+0.25$  pH units, B) pH changes, taken relative to an absolute pH of 7.4. The direction of the scans is indicated by black arrows. C-, QH- and Q-peaks are labeled. For basic pH shift (B), C-peak and QH-peak are located at  $-0.13$  V and  $0.27$  V on anodic scan, respectively. Q-peak is located at  $-0.3$  V on cathodic scan.

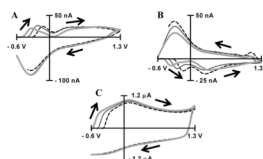


**Figure 2. Capacitive peak identification relating to pH changes**

Background-subtracted cyclic voltammograms for acidic ( $-0.25$  pH units, A) and basic ( $+0.25$  pH units, B) pH changes. Potential windows range from  $-0.6$  V (light gray line),  $-0.5$  V (dark gray line) and  $-0.4$  V (dotted black line) to  $1.3$  V. Cyclic voltammograms of background current for potential windows starting from  $-0.6$  V (light gray line),  $-0.5$  V (dark gray line) and  $-0.4$  V (dotted black line) to  $1.3$  V (C). Cyclic voltammograms were recorded at scan rate of  $400 \text{ V s}^{-1}$  in PBS buffer at pH 7.4.

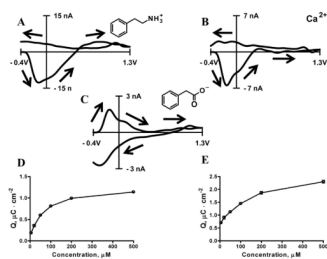


**Figure 3. Adsorption of electrochemically inert species at carbon-fiber microelectrodes**  
Background subtracted cyclic voltammogram for 20  $\mu\text{M}$  of  $\beta$ -phenylethylamine (A), 20  $\mu\text{M}$   $\text{Ca}^{2+}$  (B) and 20  $\mu\text{M}$  phenylacetic acid (C). The dependence of adsorption-induced changes in background charge from  $\beta$ -phenylethylamine (D) and  $\text{Ca}^{2+}$  (E). All cyclic voltammograms are the average of 5 voltammograms recorded for a 5 second bolus injection. Cyclic voltammograms were recorded at scan rate of 400V s<sup>-1</sup> in PBS buffer at pH 7.4.

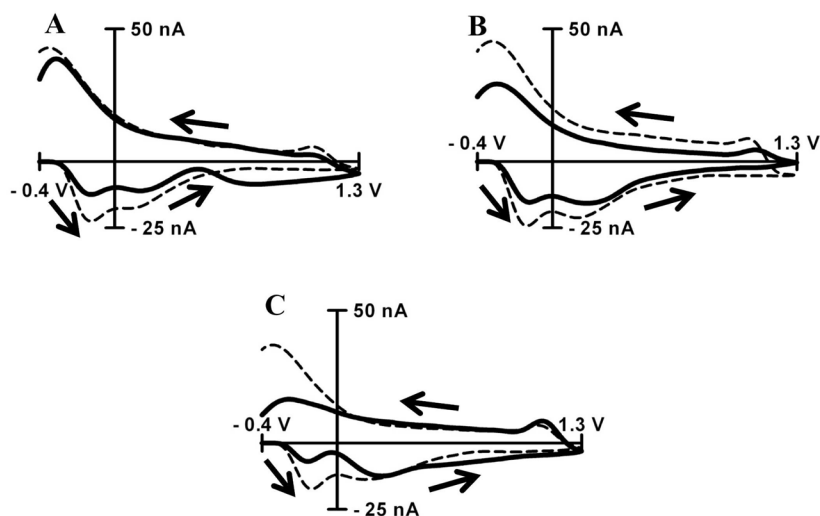


**Figure 4. Interference from adsorptive species to background subtracted cyclic voltammograms for pH**

Background subtracted cyclic voltammograms for basic pH shift (+0.25) in PBS (dashed thin trace) and in the presence of electrochemically inert species (solid thick trace). Species of interference are  $\beta$ -phenylethylamine at 500  $\mu\text{M}$  (A),  $\text{Ca}^{2+}$  at 500  $\mu\text{M}$  (B), or TRIS at 15 mM (C). Cyclic voltammograms were recorded at scan rate of  $400\text{V s}^{-1}$  in PBS buffer at pH 7.4.

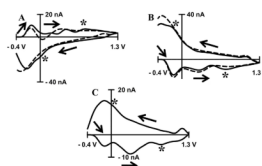


**Figure 5. The effect of DOPAC adsorption on the background-subtracted pH change cyclic voltammogram**

The presence of DOPAC (20  $\mu\text{M}$ ) significantly distorts background-subtracted cyclic voltammograms for acidic ( $-0.25$  pH units, A) and basic pH change ( $+0.25$  pH units, B). Cyclic voltammograms for pH shifts without DOPAC (dashed line) and with DOPAC (solid line). The cyclic voltammogram for basic pH shift in presence of DOPAC resembles certain cyclic voltammograms for pH shift recorded in brain in vivo (C). The extra peaks are marked with asterisks. Arrows show the direction of the scan. In vitro cyclic voltammograms were recorded at a scan rate of  $400\text{V s}^{-1}$  in PBS buffer at pH 7.4. In vivo cyclic voltammograms were recorded in nucleus accumbens after electrical stimulation of dopaminergic neurons.

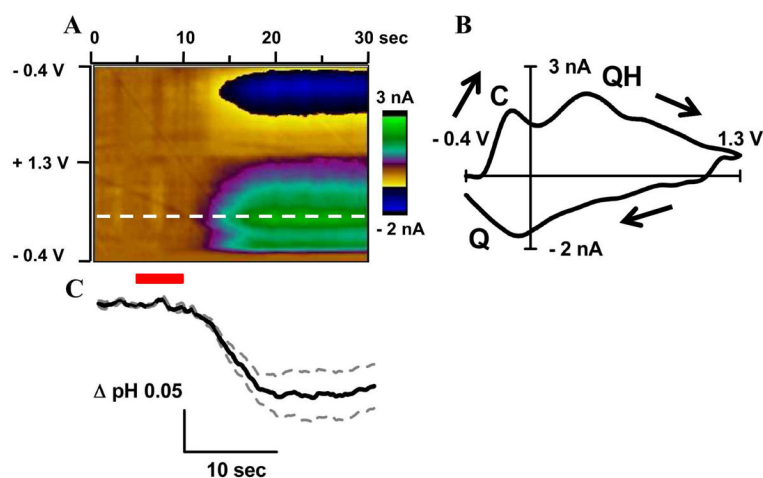


**Figure 6. Monitoring of brain acidosis induced by hypercapnia in vivo with FSCV on carbon-fiber microelectrodes**

Color plot for an acidic pH change induced by the change of a breathing mixture from air to CO<sub>2</sub> (A). Red bar marks 5 sec of CO<sub>2</sub> application. Dotted white line shows potential at which current trace for QH-peak was taken. Cyclic voltammogram recorded after hypercapnia induced acidosis reached maximum and stabilized (from 20 to 30 sec). C-peak, QH-peak (on the forward scan) and Q-peak (on the backward scan) are labeled (B). Time course of pH change obtained for QH-peak (C). Thick black solid line represents the mean and thin gray dashed lines represent standard error of the mean. Data were collected in different animals and pooled together (3 animals, 9 trials total).